

ORIGINAL ARTICLE

## Histologic comparison of microscopic treatment zones induced by fractional lasers and radiofrequency

MIN-KYUNG SHIN, JEONG HWEE CHOI, SOO BEOM AHN & MU HYOUNG LEE

Department of Dermatology, College of Medicine, Kyung Hee University, Seoul, Republic of Korea

### Abstract

**Introduction:** Fractional photothermolysis induces microscopic, localized thermal injury in the skin surrounded by undamaged viable tissue in order to promote wound healing. **Objective:** This study evaluated acute histologic changes following each single pass of various fractional lasers and radiofrequency (RF). **Methods:** Three male domestic swine were used. We used fractional Erbium:glass (Er:glass), Erbium:yttrium-aluminum-garnet (Er:YAG), CO<sub>2</sub> lasers, and fractional ablative microplasma RF. We analyzed features and average values of the diameter, depth, and vertical sectional areas treated with each kind of laser and RF. **Results:** The microscopic treatment zone (MTZ) of fractional Er:glass resulted in separation of dermoepidermal junction with no ablative zone. Fractional Er:YAG provided the most superficial and broad MTZ with little thermal collateral damage. Fractional CO<sub>2</sub> resulted in a narrow and deep “cone”-like MTZ. Fractional RF resulted in a superficial and broad “crater”-like MTZ. **Conclusions:** This study provides the first comparison of MTZs induced by various fractional lasers and RF. These data provide basic information on proper laser and RF options. We think that these findings could be a good reference for information about fractional laser-assisted drug delivery.

**Key Words:** ablative fractional laser, laser channel, microscopic treatment zone, non-ablative fractional laser

### Introduction

Fractional photothermolysis (FP) induces microscopic thermal wounds in the skin that are adjacent to undamaged viable tissue, which promotes wound healing. Both CO<sub>2</sub> and Erbium:yttrium-aluminum-garnet (Er:YAG) lasers can be associated with prolonged post-operative healing, including persistent erythema, post-inflammatory pigmentary alteration, and scarring. On the other hand, non-ablative dermal remodeling has a favorable adverse effect profile, but has limited efficacy. FP was originally developed for skin rejuvenation to fill in the gap between ablative skin resurfacing and non-ablative dermal remodeling, since ablative skin resurfacing is highly effective but is associated with a high rate of adverse effects. Fractional laser is classified into ablative and non-ablative types, subdivided depending on the laser type and wavelength. FP was applied using non-ablative near-infrared wavelengths (1.410–1.550 nm), creating vertical zones of thermal injury. Ablative fractional resurfacing was described using far-infrared wavelengths (2.940–10.600 nm), which

are highly absorbed by water and thus create vertical ablated laser channels, the so-called “microscopic ablation zones.” More recently, fractional devices have been developed to allow treatment of the face with fractional radiofrequency (RF) to provoke plasma sparks (1). However, the studies regarding the histologic differences of microscopic treatment zones (MTZs) treated by these fractional lasers and RF are limited.

Fractional lasers are used in the treatment of skin textural abnormalities (acne scarring (2), rhytides, and skin mottling associated with photoaging). Recently, fractional lasers have been used as a new method for the treatment of striae (3), female pattern hair loss (4), and drug penetration (5). In the literature, there are only a few previous histologic comparison studies that quantify lesion dimensions after fractional lasers and RF.

The MTZ acts as a microchannel to improve drug absorption through the skin. In photodynamic therapy, fractional laser has been used to facilitate the absorption of the photosensitizer. Haedersdal

Correspondence: Mu Hyoung Lee, MD, PhD, Department of Dermatology, College of Medicine, Kyung Hee University, #1 Hoeki-Dong, Dongdaemun-Ku, 130-702, Seoul, Republic of Korea. Tel: +82-2-958-8512. Fax: +82-2-969-6538. E-mail: mhlee@khmc.or.kr

(Received 2 December 2013; accepted 13 August 2014)

ISSN 1476-4172 print/ISSN 1476-4180 online © 2014 Informa UK, Ltd.  
DOI: 10.3109/14764172.2014.957216

et al. (6) reported that after treatment with fractional CO<sub>2</sub> laser, the absorption of methyl 5-aminolevulinate increased in a porcine skin model. Yu et al. (7) showed that the fractional Er:YAG laser is useful for the percutaneous delivery of intact functional therapeutic antibodies. They suggest that controlled laser microporation provides a less invasive, more patient-friendly “needle-less” alternative to parenteral administration for the local delivery of therapeutic antibodies. In order to perform fractional laser-assisted drug delivery, it is necessary to have a histopathologic understanding of microchannels treated using various fractional devices.

Wind et al. (8) compared the formation of fibrosis after non-ablative and ablative fractional laser therapy. Ablative fractional laser therapy can induce fibrosis, whereas treatment with non-ablative fractional laser does not. Histologic information on the dimensions of the laser channels in terms of ablation depth, ablation width, coagulation, and necrosis treated using various fractional lasers is very important to dermatologists for ensuring safe and efficient treatment outcomes because it allows them to choose or combine the proper kinds of fractional lasers and RF according to indications. This report evaluates the acute histopathologic skin changes including the ablation and heat diffusion areas following each single pass of various fractional lasers and RF using in vivo porcine models.

## Materials and methods

Three male domestic swine (3–6 weeks old, weighing 8–10 kg) were used in this study. This study was approved by the Kyung Hee University Medical Center Institutional Subcommittee for Research Animal Care. Animals were anesthetized using intramuscular Telazol/Xylazine (4.4 and 2.2 mg/kg)/Rompun Zoletil 50 (tiletamine/zolazepam) and made to inhale 2.0% isoflurane in oxygen at the rate of 3.0 L/minute after fasted overnight. Test areas were demarcated, and skin was exposed to various fractional lasers and RF (Table I).

Parameters of low energy and high energy were selected based on the clinical experiences of the senior author. Density was set to 50% according to manufacturer's data. The lasers and RF were

irradiated one time with no stacking. Er:glass laser (Mosaic<sup>®</sup>, Lutronic Co., Ltd, Seoul, Korea) was used for treatment at pulse energy of 50 or 100 mJ and spot density of 50 spots/cm<sup>2</sup>, using a 10×10 mm handpiece tip in a static mode. Er:YAG laser (Action<sup>®</sup>, Lutronic Co., Ltd, Seoul, Korea) was treated at pulse energy of 8 or 16 mJ and pulse width of 250 μs, using a 9×9 mm handpiece tip with a single pulse rate. CO<sub>2</sub> laser (Pixel CO<sub>2</sub><sup>®</sup>, Alma Lasers, Ltd, Israel) was applied at a pulse energy of 50 or 100 mJ in a superpulse mode (pulse duration of 300 μs and pulse rate of 1 Hz), using a 11×11 mm handpiece tip of 9×9 pixels. RF (Legato<sup>®</sup>, Alma Lasers, Ltd, Israel) was applied at power of 50–100 W, using a rolling tip handpiece delivering 132–242 pixel spots per cm.

Punch biopsy specimens were obtained from the treated sites. We did biopsies on the same day of treatment, 16 sites on each swine for a total of 48 sites on three swine. All biopsy samples were obtained from the back of the swine. Biopsy specimens were fixed in formalin, tissue blocks were embedded in paraffin, cut into 5–8 μm slices, mounted on standard microscope glasses, and stained using hematoxylin and eosin (H&E). Autofluorescence (AF) images were obtained through 6-mm snap-frozen punch biopsies at vertical sections. Tissue samples were embedded in tissue-freezing medium (Tissue-Tek Sakura Finetek Europe B.V., Zoeterwoude, the Netherlands) and frozen in liquid nitrogen. A Nuance<sup>®</sup> multispectral imaging system provided spectral data from 420 to 720 nm in 10-nm steps (CRI Instruments, Cambridge, Mass, USA). The objective lens was a Nikon PlanFluor 100× (N.A. = 1.30). Illumination was through a “DAPI” filter cube set (excitation = 358 nm; emission = 450–720 nm) (Chroma Technologies, Rockingham, Vt, USA). We analyzed 48 tissue samples in total, obtaining two tissue samples from each of the three swine, depending on the types and intensities of the lasers and RF.

The average value was measured in the intact MTZ selected in the photomicrographs. The selected sites of each skin sample were captured using an Imagescope (Coolpix 950, Nikon, Japan). The obtained photomicrographs were then analyzed using Image J software (<http://rsb.info.nih.gov/ij>).

Table I. Summary of fractionated laser devices used in this study.

Classification	Type	System	Wavelength (nm)	Manufacturer	Energy
Non-ablative fractional laser	Erbium: Glass	Mosaic <sup>®</sup>	1550	Lutronic	Low-50 mJ High-100 mJ
Ablative fractional laser	Erbium: YAG	Action <sup>®</sup>	2940	Lutronic	Low-8 mJ High-16 mJ
	CO <sub>2</sub>	Pixel CO <sub>2</sub> <sup>®</sup>	10600	Alma	Low-50 mJ High-100 mJ
Radiofrequency	RF	Legato <sup>®</sup>	RF	Alma	Low-50 W High-100 W

Table II. Average values (SD) of the diameter, depth, and vertical-sectional area in microscopic treatment zones.

Classification	Type	Energy	Total MTZ			Ablative zone			Thermal coagulative zone width
			Diameter	Depth	Area	Diameter	Depth	Area	
Non-ablative fractional laser	Erbium: Glass	Low-50 mJ	218.8	312.69	45096.86	N/A	N/A	N/A	N/A
		High-100 mJ	335.68	324.27	75787.89	N/A	N/A	N/A	N/A
Ablative fractional laser	Erbium: YAG	Low-8 mJ	N/A	N/A	N/A	267.6	45.95	10079	N/A
		High-16 mJ	242.92	76.15	14392	218.57	63.47	10219.89	23.94
	CO <sub>2</sub>	Low-50 mJ	367.02	290.28	69661.2	197.53	129.79	12873	131.03
		High-100 mJ	391.62	567.7	151667.6	166.9	348.9	30568.6	217.16
Radiofrequency	RF	Low-50 W	351	182.74	52442.43	222.34	84.47	14043	48.36
		High-100 W	395.87	172.12	54665	245.61	118.43	22923.7	57.8

*Measurements and volume calculations*

We classified MTZs which were divided into the ablative zone and thermal modified zone. For each MTZ, the following parameters were quantified: diameter, depth, and vertical sectional area. The diameters for all MTZs were measured consistently at the stratum corneum.

*Statistics*

The means and standard deviations were recorded and plotted using a standard software program (Microsoft Excel, 2003).

**Results**

We used four kinds of fractional lasers and RF, and analyzed the averages (standard deviation, SD) of the diameter, depth, and area of tissues treated with each kind. The average values are illustrated in Table II and Figure 1.

*Non-ablative fractional laser*

Fractional low-energy Er:glass laser showed that the diameter, depth, and vertical sectional area of total MTZs were 218.80 (30.51) μm, 312.69 (44.44) μm, and 45096.86 (8023.07) μm<sup>2</sup>, respectively (Table II). High-energy Er:glass showed that the diameter, depth, and vertical sectional area of total MTZs were 335.68 (59.59) μm, 324.27 (71.12) μm, and 75787.89 (21750.95) μm<sup>2</sup>, respectively.

*Ablative fractional laser*

Fractional low-energy Er:YAG laser showed that the diameter, depth, and vertical sectional area of the ablative zone were 267.60 (3.10) μm, 45.95 (7.00) μm, and 10079.00 (3503.00) μm<sup>2</sup>, respectively. High-energy Er:YAG showed that the diameter, depth, and vertical sectional area of the ablative zone were 218.57 (93.29) μm, 63.47 (15.74) μm, and 10219.89 (4682.06) μm<sup>2</sup>, respectively; the width of the coagulative zone was 23.94 (3.10) μm; the diameter, depth, and vertical sectional area of the

total MTZs were 242.92 (88.67) μm, 76.15 (22.83) μm, and 14392.00 (7397.98) μm<sup>2</sup>, respectively.

With the fractional CO<sub>2</sub> laser, the epidermis and part of the dermis demonstrated columns of thermal coagulation that surrounded tapering ablative zones lined by a thin eschar layer (Figure 2E and F). Low-energy CO<sub>2</sub> showed that the diameter, depth, and vertical sectional area of the ablative zone were 197.53 (81.32) μm, 129.79 (66.76) μm, and 12873 (4749.56) μm<sup>2</sup>, respectively; the width of the coagulative zone was 131.03 (28.58) μm; the diameter, depth, and vertical sectional area of total MTZs were 367.02 (37.3) μm, 290.28 (99.27) μm, and 69661.2 (18652.28) μm<sup>2</sup>, respectively. High-energy CO<sub>2</sub> showed that the diameter, depth, and vertical sectional area of the ablative zone were 166.90 (32.58) μm, 348.90 (147.29) μm, and 30568.60 (8702.56) μm<sup>2</sup>, respectively; the width of the coagulative zone was 217.16 (69.98) μm; the diameter, depth, and vertical sectional area of total MTZs were 391.62 (61.43) μm, 567.70 (142.98) μm, and 151667.60 (25420.72) μm<sup>2</sup>, respectively.

*Fractional ablative microplasma RF*

Fractional low-energy RF showed that the diameter, depth, and vertical sectional area of the ablative zone were 222.34 (54.41) μm, 84.47 (27.45) μm, and 14043.00 (5858.44) μm<sup>2</sup>, respectively; the width of coagulative zone was 48.36 (18.05) μm; the diameter, depth, and vertical sectional area of total MTZs were 351.00 (92.39) μm, 182.74 (81.87) μm, and 52442.43 (32551.03) μm<sup>2</sup>, respectively. High-energy RF showed that the diameter, depth, and vertical sectional area of ablative zones were 245.61 (80.56) μm, 118.43 (39.40) μm, and 22923.70 (13935.15) μm<sup>2</sup>, respectively; the width of the coagulative zone was 57.80 (29.21) μm; the diameter, depth, and vertical sectional area of total MTZs were 395.87 (86.77) μm, 172.12 (59.47) μm, and 54665.00 (30886.42) μm<sup>2</sup>, respectively.

*AF*

For the CO<sub>2</sub> and RF, areas of increased AF were observed around the ablative zone. We did not detect any visible AF changes in the Er:YAG and Er:glass.

J Cosmet Laser Ther Downloaded from informahealthcare.com by Tel Aviv University on 12/11/14 For personal use only.

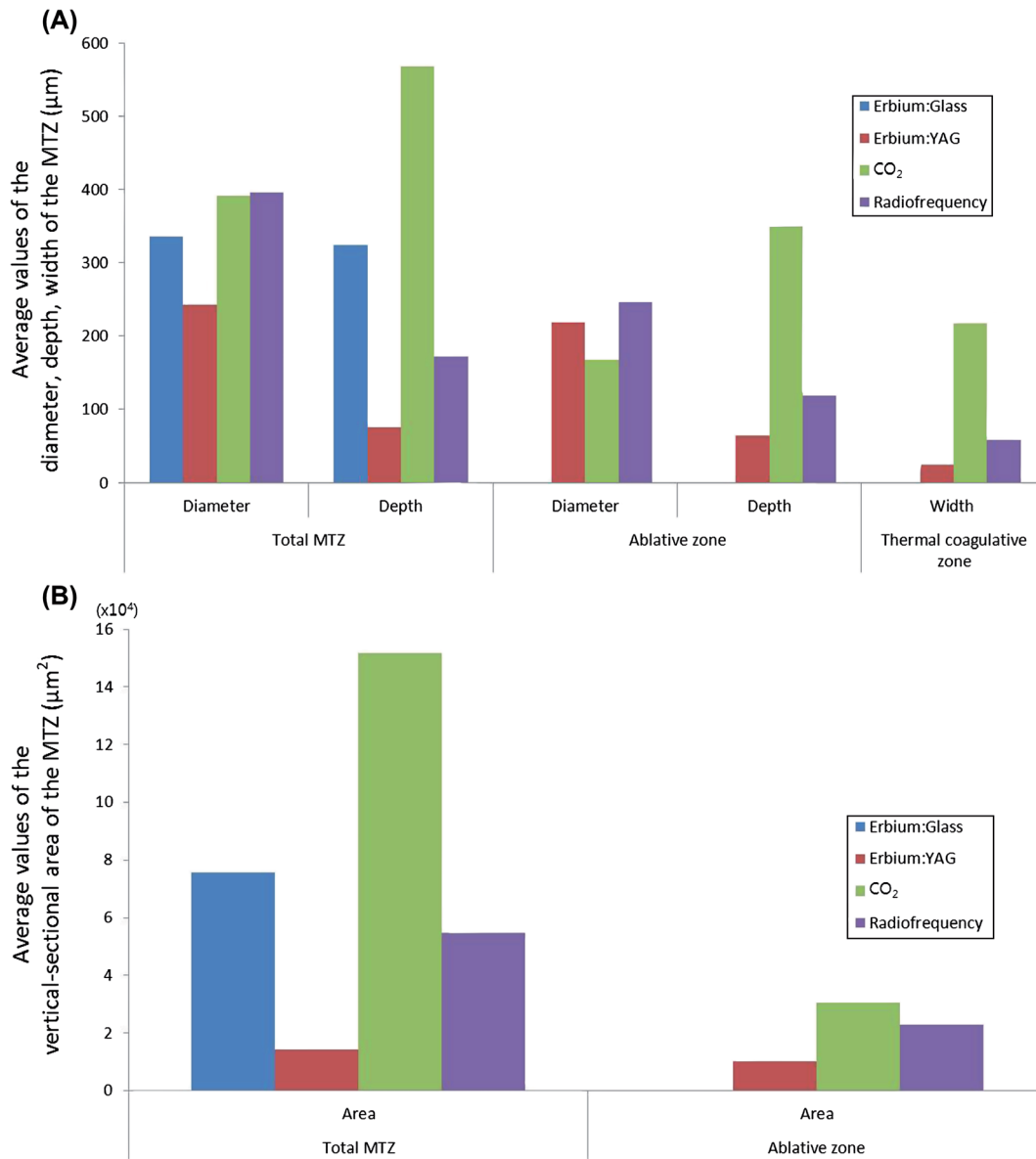


Figure 1. Average values of the diameter, depth, width, and vertical sectional area in MTZs, with high energy. (A) Diameter, depth, and width of the MTZ, (B) vertical sectional area of the MTZ.

For the RF, we observed the most obvious AF change. Figure 3 demonstrates the strong AF surrounding the ablative zone, which peaked at 550 nm.

**Discussion**

Clinical trials have been conducted to develop more effective treatments by combining various fractional lasers. Cho et al. (9) reported treating acne scars with a combined fractional laser treatment using 1550 nm Er:glass and CO<sub>2</sub> lasers. Mittelman et al. (10) reported increased patient satisfaction for facial rejuvenation with combined fractionated CO<sub>2</sub> and low-power Er:YAG laser treatments. Tenna et al. (11) treated acne scars with a combined simultaneous emission of CO<sub>2</sub> laser and RF waves, which resulted in a resurfacing effect from epidermal coagulation and a deeper remodeling due to dermal denaturation.

These methods of combining fractional lasers can be planned properly based on determination of the histopathologic features of MTZs of each laser. In order to gauge the results of clinical treatment with each device, proper documentation of the histologic skin changes at distinct laser settings is essential. Information about acute injury by fractional lasers and RF will also provide guidelines to select a proper type of laser and RF based on whether the therapeutic purpose is epidermal reepithelization or dermal remodeling. In this study, when epidermal and dermal change was compared, Er:YAG showed more superficial ablation of the epidermis with little dermal change, whereas Er:glass showed more dermal thermal change with little epidermal change.

Farkas et al. (12) compared histologic findings of fractional Er:YAG and CO<sub>2</sub> ablative-type lasers. They pointed out that the amount of fractional injury

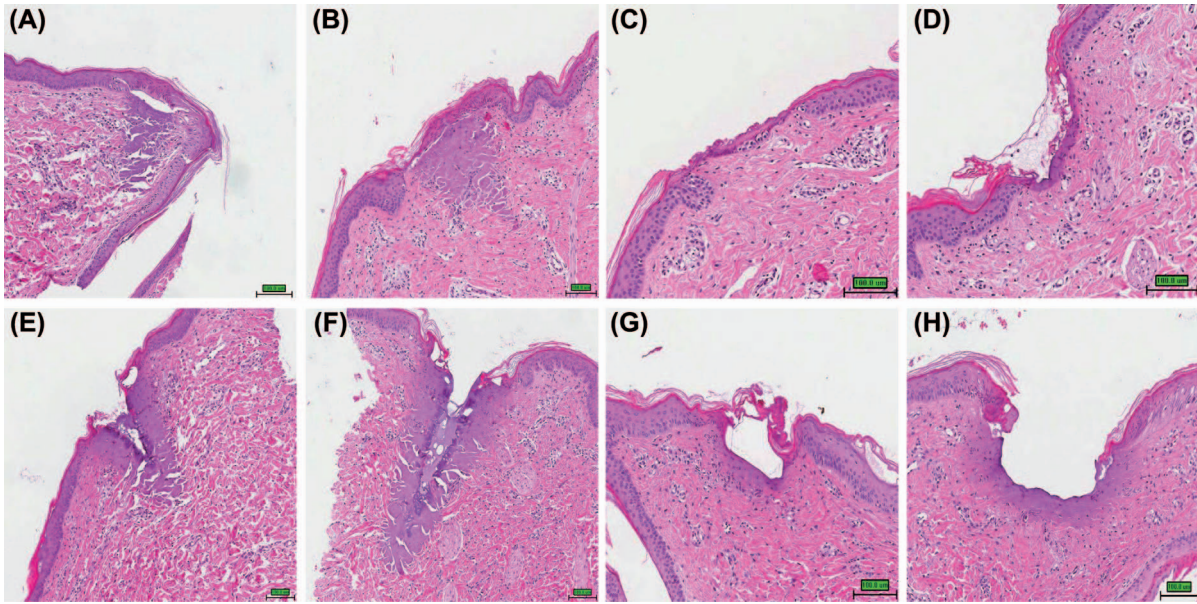


Figure 2. Histopathologic findings of various fractional lasers. (A) Low-energy Er:glass, (B) high-energy Er:glass, (C) low-energy Er:YAG, (D) low-energy Er:YAG, (E) low-energy CO<sub>2</sub>, (F) high-energy CO<sub>2</sub>, (G) low-energy RF, (H) high-energy RF (A–H, H&E, ×100).

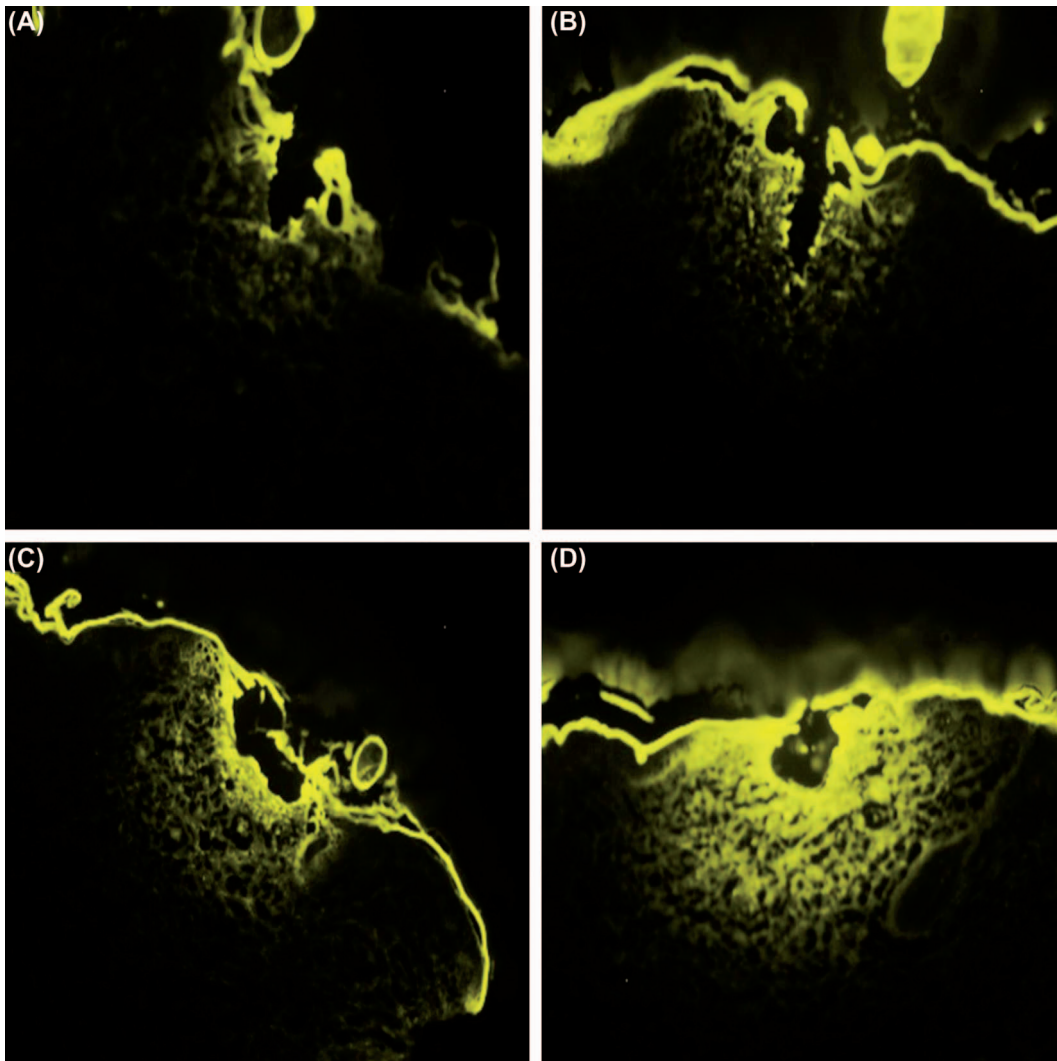


Figure 3. Strong AF surrounding the ablative zones. (A) Low-energy CO<sub>2</sub>, (B) high-energy CO<sub>2</sub>, (C) low-energy RF, (D) high-energy RF (A–D, Cryosection, ×100).

following treatment with the Er:YAG and CO<sub>2</sub> devices was markedly different. They showed that Er:YAG created the clear “punched out” ablation craters without any identifiable surrounding cellular injury. Using fractional CO<sub>2</sub>, collateral thermal injury was more extensively treated with slow repetition rates when compared with areas that were treated with faster repetition rates at similar energies. In our study, ablative craters of “punched out” appearance were observed in fractional Er:YAG and RF. Fractional RF caused stronger ablation and collateral thermal damage than Er:YAG.

We found that for fractional CO<sub>2</sub>, the depth of the total MTZ, rather than the diameter, tended to increase according to the increase in energy. Skovbolting Haak et al. (13) analyzed the microchannel induced by fractional CO<sub>2</sub> laser using an ex vivo pig skin model. They found distinct associations between the applied laser energies and the dimensions of the laser channels such that the ablation depth and the dermal ablation width increased according to increased energy levels. However, with regard to epidermal ablation width, they did not find a consistent relationship to the applied energy levels. Our study results support the conclusion that increasing the energy of fractional CO<sub>2</sub> treatment increases the depth of MTZ, and adjusting the pass or treatment repetition rates increases the coverage area of treatment. However, increasing the energy of the Er:glass or RF increased the diameter of MTZ, rather than the depth.

In this study, the widest diameter values of ablation were observed with fractional Er:YAG. Kist et al. (14) evaluated the histologic effects of a 2,940-nm fractional Er:YAG laser. They reported that the depth of ablation attained did not accurately reflect the three different laser settings. Depth of denaturation also failed to increase with increased coagulation level settings as expected. The width of ablation in the MTZ, a non-adjustable setting, was the most accurate and reproducible in all subjects. They reported that the adjustable laser depth and coagulation settings did not produce predictable depths of ablation or denaturation, possibly due to the variation in tissue hydration properties among individuals. Likewise, in our study, the MTZs of fractional Er:YAG showed the most variable values. Electrical skin–laser interactions, like tissue hydration, can affect the MTZs of fractional RF. Relatively diverse histologic appearances of MTZs within the same energy of fractional RF were observed.

Histopathologically, MTZs of fractional Er:glass showed separation of the dermoepidermal junction with no ablative zones. The MTZ of fractional Er:YAG was the most superficial and broad with little thermal collateral damage. In fractional CO<sub>2</sub> and RF, relatively deep ablative zones were observed, and fractional RF displayed superficial and broad “crater”-like microchannels; fractional CO<sub>2</sub> displayed

narrow and deep “cone”-like microchannels. CO<sub>2</sub> showed the greatest ablation depth, so this may be the most useful fractional laser for drug delivery. However, the adverse effect of thin eschars and exudations in the microchannels of CO<sub>2</sub> on drug delivery should be further investigated.

Animal studies have shown an inverse relationship between collagen fluorescence and temperature due to protein denaturing (15). Starnes et al. (16) reported that after non-ablative fractional laser treatment using 1550-nm erbium-doped fiber laser irradiation, they observed a loss of fluorescence in the extracellular matrix. In our study, AF was detected in cryosections with no staining. We observed an increase in thermal fluorescence around microchannels with a decrease in AF in the background dermal extracellular matrix. These changes were not obvious in the non-ablative fractional type. However, in the ablative fractional type, there was intense thermal fluorescence around the ablation site compared with dermal extracellular matrix AF. The use of thermal energy has been proposed as a means of shrinking redundant or lax connective tissues through collagen denaturation. When collagen is heated, the heat-labile intramolecular crosslinks are broken, and the protein undergoes a transition from a highly organized crystalline structure to a random, gel-like state (denaturation) (17). Collagen shrinkage occurs through the cumulative effect of the unwinding of the triple helix due to the destruction of the heat-labile intramolecular crosslinks and the residual tension of the heat-stable intermolecular crosslinks (17,18). Their photolability to wavelengths reaching the dermis may result in pathological conditions, particularly from thermal changes. Dermal emission and photochemical fluorescent fading behavior of these fluorophores may also serve as image findings reflective of collagen conformation, chemical behavior, excited-state properties, and supramolecular structure (15,19). We propose that these results reflect collagen denaturation characteristics, but further research is needed. Through the AF study, we sought to understand the thermal effect of the lasers. In this study, although both Er:YAG and CO<sub>2</sub> lasers are ablative types, the results diverged. As previously mentioned, in the CO<sub>2</sub> laser, areas of increased AF were observed. However, in the Er:YAG laser, we did not detect any visible AF changes. Considering these findings, we think that the CO<sub>2</sub> laser has a greater thermal effect on the tissues than the Er:YAG laser. Further investigations into changes in AFs after lasers and RF–skin interactions will be helpful for obtaining information about thermal change.

Our study has several limitations. In this report, we focused on the acute histopathologic changes after a single pass of various fractional lasers and RF. We highlighted the immediate tissue responses following treatment with these devices, and the results do not constitute a clinical report. More research is

needed to address appropriate time period and laser parameters (spot size, pulse width, energy, repetition rate, number of pulses, pulse stacking, and density).

In conclusion, these findings provide the first comparative report of MTZs which were induced by various fractional lasers and RF on the skin. These data provide basic information on appropriate laser and RF options. We believe that this report could be used as a good reference for information about combined fractional laser and drug channels. Analysis of AF following treatment with these devices can further improve our understanding of the lasers and RF-tissue interaction.

**Declaration of interest:** The authors report no declaration of interests. The authors alone are responsible for the content and writing of the paper.

## References

- Halachmi S, Orenstein A, Meneghel T, Lapidot M. A novel fractional micro-plasma radio-frequency technology for the treatment of facial scars and rhytids: a pilot study. *J Cosmet Laser Ther* 2010;12:208–212.
- Ong MW, Bashir SJ. Fractional laser resurfacing for acne scars: a review. *Br J Dermatol* 2012;166:1160–1169.
- Alexiades-Armenaka M, Sarnoff D, Gotkin R, Sadick N. Multi-center clinical study and review of fractional ablative CO2 laser resurfacing for the treatment of rhytides, photoaging, scars and striae. *J Drugs Dermatol* 2011;10:352–362.
- Lee GY, Lee SJ, Kim WS. The effect of a 1550 nm fractional erbium-glass laser in female pattern hair loss. *J Eur Acad Dermatol Venereol* 2011;25:1450–1454.
- Haedersdal M, Katsnelson J, Sakamoto FH, Farinelli WA, Doukas AG, Tam J, Anderson RR. Enhanced uptake and photoactivation of topical methyl aminolevulinate after fractional CO2 laser pretreatment. *Lasers Surg Med* 2011;43:804–813.
- Haedersdal M, Sakamoto FH, Farinelli WA, Doukas AG, Tam J, Anderson RR. Fractional CO(2) laser-assisted drug delivery. *Lasers Surg Med* 2010;42:113–122.
- Yu J, Kalaria DR, Kalia YN. Erbium:YAG fractional laser ablation for the percutaneous delivery of intact functional therapeutic antibodies. *J Control Release* 2011;156:53–59.
- Wind BS, Meesters AA, Kroon MW, Beek JF, van der Veen JP, van der Wal AC, et al. Formation of fibrosis after nonablative and ablative fractional laser therapy. *Dermatol Surg* 2012;38:437–442.
- Cho SB, Lee SJ, Kang JM, Kim YK, Oh SH. Combined fractional laser treatment with 1550-nm erbium glass and 10 600-nm carbon dioxide lasers. *J Dermatolog Treat* 2010;21:221–228.
- Mittelman H, Furr M, Lay PC. Combined fractionated CO2 and low-power erbium:YAG laser treatments. *Facial Plast Surg Clin North Am* 2012;20:135–143.
- Tenna S, Cogliandro A, Piombino L, Filoni A, Persichetti P. Combined use of fractional CO2 laser and radiofrequency waves to treat acne scars: a pilot study on 15 patients. *J Cosmet Laser Ther* 2012;14:166–171.
- Farkas JP, Richardson JA, Burrus CF, Hoopman JE, Brown SA, Kenkel JM. In vivo histopathologic comparison of the acute injury following treatment with five fractional ablative laser devices. *Aesthet Surg J* 2010;30:457–464.
- Skovbolling Haak C, Illes M, Paasch U, Haedersdal M. Histological evaluation of vertical laser channels from ablative fractional resurfacing: an ex vivo pig skin model. *Lasers Med Sci* 2011;26:465–471.
- Kist DA, Elm CM, Eleftheriou LI, Studer JA, Wallander ID, Walgrave SE, Zelickson BD. Histologic analysis of a 2,940 nm fractional device. *Lasers Surg Med* 2011;43:79–91.
- Menter JM. Temperature dependence of collagen fluorescence. *Photochem Photobiol Sci* 2006;5:403–410.
- Starnes AM, Jou PC, Molitoris JK, Lam M, Baron ED, Garcia-Zuazaga J. Acute effects of fractional laser on photoaged skin. *Dermatol Surg* 2012;38:51–57.
- Flory PJ, Garrett GR. Phase transitions in collagen and gelatin systems. *J Am Chem Soc* 1958;80:4836–4845.
- Allain JC, Le Lous M, Cohen S, Bazin S, Maroteaux P. Isometric tensions developed during the hydrothermal swelling of rat skin. *Connect Tissue Res* 1980;7:127–133.
- Menter JM, Chu EG, Martin NV. Temperature dependence of photochemical fluorescence fading in Skh-1 hairless mouse collagen. *Photodermatol Photoimmunol Photomed* 2009;25:128–131.